Cytokine-like protein 1–induced survival of monocytes suggests a combined strategy targeting MCL1 and MAPK in CMML

Margaux Sevin, Lucie Laplane, Franck Debeurme, Séverine Badel, Margot Morabito, Hanna Newman, Miguel Torres-Martin, Qin Yang, Bouchra Badaoui, Orianne Wagner-Ballon, et al.

Version of Record: https://www.sciencedirect.com/science/article/pii/S0006497121005796
Manuscript_753946f0dfb36eeada03937567e75514

Cytokine-like protein 1-induced survival of monocytes suggests a combined strategy targeting MCL1 and MAPK in CMML

Running head: Monocyte resistance to apoptosis in CMML

Margaux Sevin,[1*] Franck Debeurme,[1*] Lucie Laplane,[2] Séverine Badel,[1] Margot Morabito,[1] Hanna L Newman,[3] Miguel Torres-Martin,[4] Qin Yang,[5] Bouchra Badaoui,[6] Orianne Wagner-Ballon,[6,7] Véronique Saada,[8] Dorothée Sélimoglu-Buet,[1] Laurence Kraus-Berthier,[9] Sébastien Banquet,[9] Alix Derreal,[9] Pierre Fenaux,[10] Raphael Itzykson,[11] Thorsten Braun,[12] Gabriel Etienne,[13] Celine Berthon,[14,15] Sylvain Thepot,[16] Oliver Kepp,[17,18] Guido Kroemer,[17,18,19,20,21] Eric Padron,[3] Maria E. Figueroa,[5,22] Nathalie Droin,[1] Eric Solary[1,23,24]

** Co-first authors*

1. INSERM U1287, Gustave Roussy Cancer Campus, Villejuif, France.
2. CNRS, UMR 8590, Université Paris I, Paris, France
3. Malignant Hematology, H. Lee Moffitt Cancer Center and Research Institute, Tampa, United States
4. Icahn School of Medicine at Mount Sinai, division of liver diseases, New-York, United States
5. Human Genetics, University of Miami Miller School of Medicine, Miami, United States
6. AP-HP, Hôpitaux Universitaires Henri-Mondor, Département d'Hématologie et Immunologie biologiques, Créteil, France
7. Université Paris Est Créteil, INSERM, IMRB, Equipe 9, F-94010 Créteil, France
8. Department of biopathology, Gustave Roussy Cancer Center, Villejuif, France;
9. Institut de Recherches Internationales Servier Oncology R&D Unit, Suresnes, France.
10. Senior Hematology Department, Hôpital Saint-Louis, Université Paris Diderot, Paris, France.
11. Department of Hematology, Hôpital Saint Louis, Université Paris Diderot, Paris, France.
12. Department of Hematology, Hôpital Avicenne, Université Paris XIII, Bobigny, France.
13. Department of Medical Oncology, Institut Bergonie, Bordeaux, France
14. Department of Hematology, Centre Hospitalier Universitaire Claude Huriez, Lille, France
15. Université de Lille, IRCL, CNRS UMR9020, INSERM U1277 – Canther, Lille, France
16. Maladies du sang, Centre Hospitalier Universitaire, Angers, France
17. Metabolomics and Cell Biology Platforms, Institut Gustave Roussy, Villejuif, France
18. Centre de Recherche des Cordeliers, Equipe labellisée par la Ligue contre le cancer, Université de Paris, Sorbonne Université, Inserm U1138, Institut Universitaire de France, Paris, France
19. Pôle de Biologie, Hôpital Européen Georges Pompidou, AP-HP, Paris, France
20. Suzhou Institute for Systems Medicine, Chinese Academy of Medical Sciences, Suzhou, China (Jiangsu 215163)
21. Karolinska Institute, Department of Women's and Children's Health, Karolinska University Hospital, Stockholm, Sweden
22. Sylvester Comprehensive Cancer Center, University of Miami Miller School of Medicine, Miami, United States
23. Department of Hematology, Gustave Roussy Cancer Center, Villejuif, France
24. Université Paris-Saclay, Faculté de Médecine, Le Kremlin-Bicêtre, France

Corresponding author

Eric Solary
INSERM U1287
Gustave Roussy Cancer Campus
114 rue Edouard Vaillant
94805 Villejuif, France
Phone: 33 1 42 11 67 26
eric.solary@gustaveroussy.fr

Metrics

Title character count: 116; Text word count: 4,067; Abstract word count: 165
6 figures, 1 table, 46 references
Supplemental material: methods, 6 figures, 4 tables,

Key points

- Monocytes that accumulate in patients with a chronic myelomonocytic leukemia have a defective apoptosis through addiction to MCL1
- Combined MCL1 and MEK inhibition restores monocyte apoptosis and decreases leukemic burden in xenografted animals

Abstract

Mouse models of chronic myeloid malignancies suggest that targeting mature cells of the malignant clone disrupts feedback loops that promote disease expansion. Here, we show that, in chronic myelomonocytic leukemia (CMML), monocytes that accumulate in the peripheral blood show a decreased propensity to die by apoptosis. BH3 profiling demonstrates their addiction to MCL1 (myeloid cell leukemia-1), which can be targeted with the small molecule inhibitor S63845. RNA sequencing and DNA methylation pattern analysis both point also to the implication of the MAPK (mitogen-activated protein kinase) pathway in the resistance of CMML monocytes to death and reveal an autocrine pathway in which the secreted cytokine CYTL1 (Cytokine-like protein 1) promotes ERK (extracellular signal-regulated kinase) activation through CCR2 (C-C chemokine receptor type 2). Combined MAPK and MCL1 inhibition restores apoptosis of CMML patient monocytes and reduces the expansion of patient-derived xenografts in mice. These results designate the combined inhibition of MCL1 and MAPK as a promising approach to slow down CMML progression by inducing leukemic monocyte apoptosis.

Introduction

Chronic myeloid malignancies are diseases of the hematopoietic stem cell (HSC) in which lineage differentiation is preserved. Mature myeloid cells of the malignant clone contribute to disease development, as demonstrated in a mouse model of chronic myeloid leukemia in which BCR/ABL tyrosine kinase activity promotes overproduction of interleukin-6 (IL-6) by mature cells of the clone. In turn, IL-6 skews immature cell differentiation toward the myeloid lineage.[1] Neutralization of IL-6 blocks disease installation and progression in this model,[2] suggesting that targeting cytokine-dependent feedforward loops may constitute a new efficient therapeutic approach in chronic myeloid malignancies.

Chronic myelomonocytic leukemia (CMML) is a prototypic chronic myeloid malignancy in thus far that it associates features of myelodysplastic syndromes and myeloproliferative neoplasms.[3] This clonal disorder, mostly observed in the elderly, is associated with the stepwise accumulation of somatic mutations in epigenetic, splicing, and signaling genes in a HSC.[4] Feedback loops involving mutation-induced cytokine overproduction may exist in CMML, *eg*, *TET2* gene mutation, the most frequent somatic event in this disease, compromises the ability of the protein to downregulate *IL6* gene expression in monocytes and macrophages at the resolution phase of inflammation, thus generating an inflammatory state that drives excessive myelopoiesis.[5,6]

Due to their advanced age and comorbidities, few CMML patients are eligible for allogeneic stem cell transplantation.[7] Hypomethylating agents transiently reverse the disease phenotype in responding patients, but their genomic impact remains limited.[8] Other conventional therapies aim at attenuating symptoms by a personalized strategy to minimize cytopenia-induced or proliferation-associated symptoms.[9] These conventional therapies do not alter the natural course of this severe disease, indicating an unmet need for curative approaches. Currently tested strategies target recurrent mutations in actionable genes[4] or the unique dependence of CMML on granulocyte macrophage colony-stimulating factor (GM-CSF).[10] Theoretically, a therapeutic strategy that eliminates mature differentiation products of the malignant clone might complement these approaches.

The hallmark of CMML is a persistent peripheral blood monocytosis ≥1 × 10^9/L with monocytes accounting for ≥10% of the white blood cells.[3] Monocytes that accumulate in the

peripheral blood of CMML patients are predominantly classic monocytes with a $CD14^{+}CD16^{-}$ phenotype.[11] Virtually all these cells are generated by the leukemic clone.[12]

Here, we identify defective apoptosis of circulating classic monocytes in CMML. Resistance to apoptosis involves the BCL2-related protein MCL1 (myeloid cell leukemia-1), together with the overproduction of CYTL1 (Cytokine-like protein 1),[13] a cytokine that activates the MAPK (mitogen-activated protein kinase) signaling pathway by interacting with CCR2 (C-C chemokine receptor type 2) in an autocrine or paracrine manner. Inhibition of MCL1 using the small molecule S63845, combined with ATP-independent inhibitors of MAPK kinases (MEK1 and MEK2), either selumetinib or trametinib, restores monocyte apoptosis and decreases tissue infiltration by leukemic cells in xenografted mice. These results designate the combined inhibition of MCL1 and MEK as a therapeutic opportunity that should be evaluated for the treatment of CMML.

Patients and methods

Patient samples. Peripheral blood samples were collected from CMML patients and age-matched healthy donors in the context of a non-interventional study validated by the ethical committee Ile de France 1 (DC-2014-2091). Buffy coats were collected from young healthy blood donors (Etablissement Français du Sang, Rungis, France). CMML patients were diagnosed according to the last iteration of the World Health Organization (WHO) classification of myeloid malignancies.[3] Clinico-biological characteristics of the patients, summarized in **Table 1**, were obtained from our registered database (DR-2016-256). Peripheral blood mononuclear cells (PBMC) were sorted using density centrifugation Pancoll (Pan-Biotech, Dutscher, Brumath, France) and $CD14^+$ monocytes through negative selection with magnetic beads and the AutoMacs system (Miltenyi Biotech, Paris, France). Gene mutations were screened as described.[8,12]

Reagents. iBH3 peptides were made by Proteogenix (Schiltigheim, France). Venetoclax, navitoclax, and selumetinib (AZD-6244) were purchased from selleckchem (Munich, Germany) and trametinib from Euromedex (Souffelweyersheim, France). S63845 was synthesized by Servier.[14] Recombinant human CYTL1 was purchased from CliniSciences (Nanterre, France), CAS 445479 and RS 504393 from Sigma-Aldrich (Saint-Quentin Fallavier, France) and Tocris (Noyal Châtillon sur Seiche, France), respectively. Antibodies are listed in supplemental material.

Cell death detection. Sorted $CD14^+$ monocytes were cultured overnight in RPMI 1640 medium supplemented or not with fetal calf serum (Thermo Fisher). Cell death was identified by Trypan blue staining or by flow cytometry analysis of cells stained with annexin V-FITC and propidium iodide (PI) antibodies before flow cytometry analysis using Canto X cytometer (BD Biosciences) and analysis using FlowJo (FlowJo LLC, Ashland, Oregon).

Intracellular BH3 (iBH3) profiling. PBMCs were stained with Live/Dead Blue (Invitrogen, Cergy Pontoise, France) for 20 min on ice, then with CD45, CD24, CD14, CD16, CD2, and CD56 antibodies in MACS buffer, pelleted and suspended in DTEB (135 mM trehalose, 50 mM KCl, 20 uM EDTA, 20 uM EGTA, 5 mM succinate, 0.1% BSA, 10 mM HEPES-KOH, pH 7.5) before being exposed to peptides with 0.002% w/v digitonin as described.[15] The fraction of cytochrome c released was calculated as $100 \times (1-[(MFI_{sample}–MFI_{FMO})/(MFI_{PUMA2A}–MFI_{FMO})])$.

Confocal analysis. $CD14^+$ monocytes seeded on cover glasses were fixed in 4% paraformaldehyde, permeabilized with ethanol 70% and labeled with mouse anti-γH2AX (1:500, Millipore, Molsheim, France), rabbit anti-active caspase-3 (1:150, Cell Signaling Technology), then with Alexa Fluor 488 goat anti-mouse IgG and Alexa Fluor 555 goat anti-rabbit IgG, respectively before being analyzed as described.[16]

Gene expression analysis. Total RNA (0.5 µg) from $CD14^+$ monocytes was reverse transcribed using SuperScript VILO cDNA synthesis kit (ThermoFischer Scientific). RT-qPCR was performed with SyBR Green master mix in an Applied Biosystems 7500 thermocycler as described.[17] Data were normalized to four housekeeping genes (*PPIA, GAPDH, HPRT,* and *RPL32*; primer sequences in **table S1)**.

Immunoblotting. Cells lysed with Laemmli Buffer (5% sodium dodecyl sulfate, 10% glycerol, 32.9 mM Tris-HCl pH 6.8) supplemented with dithiothreitol 0.1 M, protease and phosphatase inhibitors (Roche) were subjected to migration, transfer and analysis according to standard protocols.

DNA methylation by Enhanced Reduced Representation Bisulfite Sequencing (ERRBS). High-molecular-weight genomic DNA (25 ng) was used to perform ERRBS, sequenced on an Illumina HiSeq 2500, and analyzed as described.[8]

RNA sequencing. $CD14^+$ monocyte RNA (integrity score ≥7.0) was used to prepare libraries with Illumina TruSeq RNA Sample Prep Kit V2 and sequence on a 75 bp pair-end run using NextSeq 500 High Output Kit as described.[16] Transcripts from Gencode V24 were quantified in transcript per million (TPM) using Kallisto software. Gene-level expression was the sum of TPM values for each gene transcript. Raw reads were mapped to hg19 genome with Tophat2 (v2.0.14)/Bowtie2 (v2.1.0). The number of reads per gene was counted using HTSeq (0.5.4p5) and GENECODE (v24lift37) and differential gene expression analysis using DESeq2 package (v1.10.1). Genes with an absolute log2 fold change > 1 and $P < 0.05$ were reported.

Chromatin immunoprecipitation (ChIP)-sequencing. ChIP experiments were performed with a ChIP-IT kit (Active Motif). Cells were cross-linked with addition of 1% formaldehyde to the culture medium for 10 min and the reaction was stopped with glycine. After lysis in SDS lysis buffer, and sonication, antibodies (5µg) were incubated overnight. Chromatin immunoprecipitated with EGR1 antibody (sc110, Santa-Cruz) was eluted from magnetic

beads before reversing cross-links. Sequencing and analysis were performed as described.[16] ChIP-PCR experiments are described in the supplemental material.

Cytokine dosage. Human plasma was obtained by peripheral blood centrifugation (180g, 10 min, then 21,000 g 5 min). CYTL1 was quantified using an ELISA (CliniSciences). Cytokines were quantified in mouse plasma using V-PLEX (Human Proinflammatory Panel II, MSD, Rockville, MD) and custom mIL-1beta, mIL-6 and mTNF-alpha (MSD).

Patient-derived xenografts (PDX). Experiments, which were approved by the Ethical Committee (2016-104-7171), were performed following two previously described methods.[18,19] Research was conducted in accordance with the Declaration of Helsinki. Details are provided in the supplemental material.

Statistics. Data are displayed as means ± SEM. Statistically significant differences were assessed using the Mann–Whitney test or Student's *t* test (2 groups) or an ANOVA (>2 groups). Similarity of variance was tested using GraphPad PRISM (San Diego, CA) before any statistical analysis. $P < 0.05$ was considered significant.

Data Sharing: Data are available under accession number GSE165305

Results

Defective apoptosis of CMML peripheral blood monocytes.

$CD14^+$ monocytes were isolated from the peripheral blood of 190 CMML patients, whose characteristics are summarized in **Table 1**, and age-matched healthy donors. These cells (CMML=16, **table S2, cohort #1**; healthy donors=27) were cultured in the absence of serum. After 4 days, virtually all the healthy donor monocytes stained positively with Trypan blue, while a variable fraction of CMML monocytes remained unstained, indicating better survival (**Figure 1A**). The death of healthy donor monocytes cultured for 24 hours in the absence or presence of serum was associated with Annexin-V (AnV) labeling (**Figure S1A**), a decrease in the mitochondrial membrane potential (**Figure S1B**), cleavage of the fluorogenic caspase substrates Ac-DEVD-AMC (**Figure S1C**) and Ac-IETD-AFC (**Figure S1D**), and cleavage of poly(ADP-ribose) polymerase (**Figure S1E**), indicating caspase-dependent apoptosis that could be prevented by the addition of 1 μM Q-VD-OPh (**Figure S1A to S1E**). The resistance of CMML monocytes to apoptosis was validated by analysis of AnV-FITC and propidium iodide (IP)–stained monocytes collected from 21 CMML patients (**Table S2, cohort #2**) and 30 age-matched healthy donors that were cultured for 4 days in serum free medium (**Figure 1B**). This resistance to apoptosis could be detected in a shorter assay in which monocytes were cultured in serum-containing medium for 24 hours. Again, CMML patient monocytes (n=78; **Table S2, cohort #3**) demonstrated a decreased frequency of apoptosis as compared to age-matched control monocytes (n=102) (**Figure 1C**). The resistance of CMML monocytes to apoptosis was further confirmed by a decreased immunofluorescence detection of nuclear γ-H_2AX and active caspase-3 (**Figure S1F**) and a decreased cleavage of Ac-DEVD-AMC fluorogenic substrate (**Figure S1G**). Of note, when explored immediately after cell sorting, no difference between healthy donors and CMML monocytes could be detected (**Figure S1H**). Clinically, no correlation was found between CMML monocyte resistance to apoptosis and WHO classification (**Figure 1D**). The increased resistance of CMML monocytes to death correlated with a higher number of *NRAS* mutations, without a significant relationship with other recurrent mutations (**Figure 1E**). Also, no correlation was detected between monocyte sensitivity to apoptosis and blood cell parameters (**Figure S1I**), with only a trend towards and an increased resistance of monocytes to apoptosis with their increasing count in the peripheral blood (**Figure S1J**). Finally, monocyte viability was similar in patients who received

hydroxyurea (HU) treatment and untreated patients (**Figure S1K**), even when monocytes of the same patients were tested before and after having initiated HU treatment (not shown). In contrast, patients who responded to a demethylating drug demonstrated a therapy-induced increase in monocytic apoptosis (**Figure S1L)**, which was not observed in non-responding patients or those with a stable disease **(Figure S1M**). Of note, we did not detect any resistance to apoptosis of CMML $CD34^+$ cells in liquid culture (**Figure S1N**).

CMML monocytes are addicted to MCL1.

To determine the molecular mechanisms through which CMML monocytes resist apoptosis, we investigated their functional dependence on specific BCL2 family members by using a BH3 profiling assay.[15] Briefly, we measured the propensity of monocytes exposed to peptides that mimic the BH3 domain of pro-apoptotic BCL-2 family members (**Table S3**) to initiate mitochondrial apoptosis, as indicated by the cytosolic release of cytochrome c. The tested peptides were selected to measure the dependency of CMML monocytes on anti-apoptotic BCL2 family members that include BCL2, $BCLX_L$, MCL1, BFL1, and BCLW (**Figure S2A**). Results obtained in 21 CMML patients (**Table S2, cohort #4**) compared with 18 age-matched healthy donors indicated that healthy donor and CMML monocytes were equally sensitive to BIM and PUMA-derived BH3 peptides. In contrast, CMML monocytes were more sensitive to NOXA- and HRK-derived BH3 peptides and their combination, suggesting an increased dependency on MCL1 and $BCLX_L$ (**Figure 2A**). Cells that were sensitive to the NOXA-derived BH3 peptide were also sensitive to the HRK-derived BH3 peptide (**Figure S2B**). RT-qPCR analysis of *BCL2* family gene expression (**Table S2, cohort # 5**, CMML, up to 30 patients) compared with age-matched healthy donors did not detect any significant change in CMML cells compared to age-matched healthy donor monocytes (**Figure 2B and S2C**). Also, immunoblotting of sorted CMML monocyte proteins (**Table S2, cohort #6**) compared to age-matched healthy donors did not detect any significant difference in BCL2, MCL1, and $BCLX_L$ protein expression (**Figure S2D and S2E**). These results indicated that the dependency of CMML monocytes on MCL1 and $BCLX_L$ could not be explained by the up-regulation of the corresponding genes and proteins. We then explored the ability of BCL2 family protein inhibitors to restore CMML monocyte apoptosis. In comparison with age-matched healthy donor monocytes, CMML cells showed an increased sensitivity to the selective MCL1

inhibitor S63845 (**Table S2, cohort #7,** CMML=89), but not to the specific BCL2 inhibitor venetoclax, nor to the BCL2, $BCLX_L$, and BCLW inhibitor navitoclax (**Figure 2C**). As observed in other cell types,[14] exposure to S63845 increased MCL1 expression in sorted monocytes (**Figure 2D**). S63845 compound also triggered PARP cleavage (**Figure 2D**), further supporting its ability to restore caspase-dependent apoptosis in CMML monocytes. Altogether, CMML monocytes appeared to be mostly addicted to the anti-apoptotic effects of MCL1.

MAPK signaling pathway activation may contribute to apoptosis resistance.

To further explore the molecular mechanisms involved in monocyte resistance to apoptosis, we segregated a cohort of 19 CMML patients into two groups, based on the fraction of dead monocyte (> or ≤50%) after 24 hours in serum containing medium. We used ERRBS to explore DNA methylation patterns in sorted monocytes collected from 10 patients with the most resistant cells (defective apoptosis) and 9 patients with less resistant cells (non-defective apoptosis) (**Figure S3A & table S2, cohort #8**), showing a limited number of differentially methylated regions between the two groups (**Figure 3A**). Pathway analysis using Gene Ontology Molecular Function identified the mitogen activated protein 3 kinase (MAP3K) pathway as the most significantly distinct between defective and non-defective CMML monocytes (**Figure 3B**). We also sequenced RNA of these sorted monocytes, identifying only 24 differentially expressed genes (**Figure 3C, figure S3B, table S2, cohort #8, and table S4**)**.** RT-qPCR analysis of samples used for RNA sequencing (compared with 11 healthy donor monocytes) validated *CYTL1* and *EREG* overexpression as well as *ITGA2B, PTK2,* and *TUBB1* downregulation in CMML monocytes with defective apoptosis compared to the two other groups (**Figure S3C**). *GLTSCR2* was the only gene whose deregulation in monocytes with defective apoptosis was not validated by RT-qPCR analysis (**Figure S3C**). We did not detect a significant overlap between differentially expressed genes and differentially methylated regions, even when focusing on topologically associating domains.

The same cut-off value (> or ≤50% monocyte survival after 24 hours in serum containing medium) was applied to an extended cohort of patients and age-matched controls, indicating that the sensitivity to apoptosis of “non-defective” monocytes was similar to that of controls (**Figure S3D**). Addition of 10% peripheral blood plasma collected from CMML patients to culture medium could improve healthy donor monocyte survival, which was not

observed with healthy donor plasma (**Figure 3D and table S2, cohort #9**). This observation suggested that one or several soluble factors present in the plasma of CMML patients could inhibit monocyte apoptosis. Based on this observation, we selected *CYTL1* among differentially expressed genes between CMML monocytes with and without defective apoptosis (**Figure 3C**). *CYTL1* encodes a small secreted protein that acts as a chemo-attractant activating the ERK pathway in human monocytes.[13] Further exploring *CYTL1* gene expression in an independent cohort of 35 CMML patients (**Table S2, cohort #10**) compared with 19 healthy donors, we validated *CYTL1* gene overexpression in CMML patients compared with healthy donor monocytes (**Figure 3E**). *CYTL1* was especially, but not exclusively associated to apoptosis resistance (**Figure S3E**). We also looked at *CYTL1* gene expression in a recently published[20] cohort of monocytes sorted from the peripheral blood of CMML patients (n=12) and young (n=16) and disease age-matched (n=12) healthy donors. Again, we observed *CYTL1* overexpression of in CMML patient monocytes compared with healthy donors of any age (**Figure 3F**). This overexpression was not observed in sorted $CD34^+$ cells, plasmacytoid dendritic cells,[21] granulocytes and bone marrow mesenchymal stromal cells (not shown). In accordance with the overabundance of *CYTL1* mRNA in CMML monocytes, CYTL1 protein measured by ELISA was significantly increased in the peripheral blood plasma of CMML patients as compared to healthy donors (**Figure 3G and table S2, cohort #11**), and this was especially significant for patients with defective apoptosis (**Figure S3F**). *CYTL1* gene expression in peripheral blood monocytes or CYTL1 protein plasma levels did not correlate with any clinical or biological CMML characteristics (not shown), indicating that CYTL1 overexpression may be independent of the other disease parameters.

CYTL1 protects human monocytes from apoptosis.

Further investigating the upregulation of *CYTL1* in monocytes of CMML patients, we analysed chromatin immunoprecipitation-sequencing (ChIP-Seq) data obtained from sorted human monocytes (H3K27me3, H3K27ac, H3K4me1, H3K4me3). In healthy donor monocytes and two CMML patient monocytes, we also immunoprecipitated the early growth response (EGR)-1 transcription factor, a well-identified target of phosphorylated ERK (p-ERK).[22] The combined deposition of H3K4me1, H3K4me3, and H3K27ac suggested the presence of an active enhancer upstream the *CYTL1* gene to which EGR1 was recruited in CMML monocytes

(**Figure 4A**), which was supported by genome-wide integration of enhancers and target genes in the framework of GeneCards (GH04J005032).[23] ChIP-PCR using two distinct set of primers further validated the enrichment of EGR1 to this enhancer is CMML samples with increased *CYTL1* gene expression as compared to healthy donor cells (**Figure 4B**). siRNA-mediated down-regulation of *EGR1*, performed in U937 cells, decreased *CYTL1* expression correlating with the decrease in *EGR1* (**Figure S4A**). Exposure of healthy donor monocytes to 100 ng/mL rhCYTL1 induced the phosphorylation of ERK in a time- and dose-dependent manner (**Figure 4C and S4B**), and this effect could be prevented with a 30 minute pre- / co-incubation with the CCR2 antagonist CAS 445479-97-0 (8 nM) (**Figure 4C**). Incubation of healthy donor monocytes in serum-free medium in the absence or presence of 100 ng/ml rhCYTL1 for 24 hours confirmed that this cytokine is capable of preventing apoptosis induced by serum deprivation (**Figure 4D**), even in low-binding plates that prevents their adhesion (**Figure S4C**). Addition of CAS 445479-97-0 (8 nM) or another CCR2 antagonist RS 504598 (10 µM) suppressed the cytoprotective effect of rhCYTL1 (**Figure 4E**). Altogether, these results suggest an autocrine or paracrine feedback loop in which CYTL1, through CCR2-mediated ERK phosphorylation, inhibits monocyte death accompanied by EGR1 recruitment to *CYTL1* gene enhancer. The expression of *CCL2* gene, which encodes another ligand for CCR2, was similar in healthy donor and CMML monocytes (**Figure S4D and S4E**).

S63845 synergizes with MEK inhibitors to restore CMML monocyte apoptosis.

Knowing that CYTL1 is overproduced in CMML and activates the MAPK/ERK (MEK) pathway in monocytes,[13] we explored the possibility that two FDA-approved orally bioavailable MEK inhibitors, namely selumetinib and trametinib, could increase CMML monocyte susceptibility to the MCL1 inhibitor S63845. The two combinations (selumetinib+ S63845 or trametinib+S63845) exhibited a synergistic ability to promote CMML monocyte apoptosis, which was more pronounced in CMML than healthy donor monocytes (**Figure 5A, 5B, and Table S2, cohort #12**). This effect could be prevented by Q-VD-OPh, suggesting caspase-dependent apoptosis, whereas necrostatin-1, which targets the pronecrotic kinase receptor interacting protein-1, did not show any protective activity (**Figure S5A**). Importantly, the two combinations, in addition to decreasing P-ERK, induced a decrease in MCL1 protein levels (**Figure 5C and 5D**) that was not observed with each of these drugs tested alone (**Figure 5D**

and 5E). These drugs showed limited effects on the survival of enriched healthy donor and CMML $CD34^+$ cells (**Figure S5B**).

S63845 combined with MEK inhibitors decreases CMML cells *in vivo*.

Finally, we used PDX models[18,19] to test the efficacy of S63845 in combination with MEK inhibitors. PDX of CMML hardly allow amplification through serial transplantation without oncogenic modification.[24] First, PDX generated from 2 patients (**Figure 6A**) were treated, 7 weeks after iv injection of CD34+ cells, with vehicle (n=12) or intravenous S63845 (20 mg/kg) once a week and daily oral AZD6244 (10 mg/kg), 5 days a week (n=15), for 3 weeks (**Figure 6B**), which induced a significant decrease in splenic size (**Figure 6B**) and weight (**Figure 6C**), as well as in the total number of $hCD45^+$ and $hCD45^+$,$CD14^+$ cells infiltrating the spleen and $hCD45^+$ in the peripheral blood (**Figure 6C**). The drug combination did not affect mouse hemoglobin levels or white blood cell counts, but significantly decreased the level of inflammatory human cytokines, including IL-1β, IL-6, IL-8 and TNFα, in the peripheral blood (vehicle, n=7; combo, n=8) (**Figure 6D**). In independent experiments, mice intravenously injected with patient cells were treated with the combination of intravenous S63845 (once per week) or oral trametinib (1.0 mg/kg, 5 days per week) or their combination for 3 weeks (**Figure 6E and S6**). The combination induced a significant decrease in splenic weight and the total number of human cells infiltrating the spleen and in peripheral blood (**Figure 6E**). This PDX model mimics monocyte patient sensitivity to the tested drugs *ex vivo*, *i.e.* S63845 efficacy was not increased in this patient cells by the combination to Trametinib (not shown). Analysis of two additional PDX models showed a better efficacy of the combination in decreasing bone marrow hCD45+ cells (**Figure S6**). Together, these results demonstrate the MCL1 / MEK inhibitor combination ability to reduce CMML leukemic cell burden *in vivo*.

Discussion

This study identifies an MCL1/MEK-dependent inhibition of monocyte apoptosis in CMML, which involves a CYTL1- and CCR2-mediated autocrine or paracrine loop. Simultaneous inactivation of MCL1 and MEK efficiently decreases leukemic burden and the generation of inflammatory cytokines in PDX models, suggesting a novel therapeutic approach to slow down CMML progression.

Monocytes that accumulate in CMML patients are frequently addicted to MCL1, an anti-apoptotic protein of the BCL2 family that was initially detected in leukemic cells undergoing monocyte differentiation.[25,26] While *MCL1* gene expression is increased in many tumor types,[27,28] CMML monocytes that resist apoptosis do not show an overexpression of the gene or the protein, yet are more dependent on MCL1 than healthy donor monocytes. This resistance is not an intrinsic property of the classical monocyte subset whose increased fraction characterizes the disease and may be the consequence of genetic and epigenetic events involved in disease generation and progression.[29]

The resistance of CMML monocytes to apoptosis is not S63845 is a selective and potent small-molecule MCL1 antagonist that demonstrated impressive preclinical activity against selected tumors and little toxicity in mouse models.[14] BH3 mimetics activity is commonly optimized by combination with other agents.[29-36] Analysis of DNA methylation pattern and gene expression in CMML monocyte samples pointed to MAP3K pathway activation in apoptosis-resistant cells, suggesting that MEK inhibitors could enforce the ability of MCL1 inhibitors to restore CMML monocyte apoptosis.

Among the genes whose expression was increased in apoptosis-resistant CMML monocytes, *CYTL1* overexpression was validated in several independent cohorts of patients. *CYTL1* gene could be slightly more expressed in CMML compared to reactive monocytes but the small size of the cohort precluded any definitive conclusion. Initially cloned in human $CD34^+$ cells,[37] this conserved gene encodes a small secreted protein[38] with a cytokine-like structure[38,39] resembling CCL2. CYTL1 could bind with high affinity to the receptor of CCL2 and other chemokines known as CCR2 at the surface of monocytes and macrophages.[13] While CMML monocytes do not overexpress *CCL2* gene, the cytokine can be increased in the plasma of CMML patients[40] and may further promote the resistance to apoptosis of CMML monocytes.

Antagonizing CCR2 with inhibitors that are currently tested in the treatment of diabetes mellitus,[41] cancer,[42] and HIV1 infection[43] could be an alternative to MEK inhibitors to promote the MCL1 inhibition efficacy in CMML.

Increasing evidence indicates a causative role of inflammation in the pathogenesis of myeloid malignancies.[44] Anti-inflammatory drugs targeting the IL6/STAT3 pathway inhibit the survival advantage provided by *Tet2* gene deletion in mouse HSCs.[6] In PDX models of CMML, the combination of MCL1 and MEK inhibitors decreased the secretion of human inflammatory cytokines IL1β, IL-6, IL-8 and TNFα, which are part of the inflammatory secretome identified in CMML patients.[40] Restoring apoptosis of CMML monocytes might inhibit the production of inflammatory cytokines that contribute to disease progression through interaction with normal and leukemic stem cells.[20]

Recovering of apoptosis could account for the clinical impact of hypomethylating agents that otherwise fail to decrease mutational burden.[8] In contrast, hydroxyurea does not improve monocyte apoptosis, indicating a distinct mode of action as compared with MCL1 inhibitors. Since *Mcl1*$^{+/-}$ heterozygous mice tolerate cytotoxic drugs at clinically relevant doses,[45] the combination of MCL1 inhibitors with standard chemotherapy remains a therapeutic option.

Altogether, defective apoptosis in CMML monocytes involves MCL1 and MEK pathway activation through the cytokine-like CYTL1 interacting with CCR2 in an autocrine or paracrine loop. These results, which further validate MEK pathway as a potential therapeutic target in CMML,[24,46] suggest innovative therapeutic options to explore in this disease. As soon as ongoing trials will demonstrate the innocuousness of these drugs, such a combination will deserve to be clinically tested.

Acknowledgements

This work was supported by a grant from Servier laboratories in the context of the Molecular Medicine in Oncology program led by Gustave Roussy Institute (IHU-B program, Agence Nationale de la Recherche). ES and GK are supported by the Ligue contre le Cancer (équipes labellisées); ES is supported by the Fonds Amgen France pour la Science et l'Humain and the Institut National du Cancer (INCa); GK is supported by Agence National de la Recherche (ANR) – Projets blancs; Cancéropôle Ile-de-France; Institut National du Cancer (INCa); Inserm (HTE); Institut Universitaire de France; the LabEx Immuno-Oncology (ANR-18-IDEX-0001); the RHU Torino Lumière; the SIRIC Stratified Oncology Cell DNA Repair and Tumor Immune Elimination (SOCRATE); and the SIRIC Cancer Research and Personalized Medicine (CARPEM). This study contributes to the IdEx Université de Paris ANR-18-IDEX-0001.

Authorship contributions

Conceptualization, ES; Methodology, FD, GK, MEF, ND, ES; Investigation, MS, FD, MM, MTM, DSB, OK, ND; Formal analysis, LL, MTM, MEF, ND, ES; Funding acquisition, ES; Resources, BB, OWB, VS, LKB, SB, AD, PF, RI, TB, GE, CB, ST; Data curation, MS, ES; Validation, ES; Visualization, ; Writing – Original Draft, ES; Writing, review, editing, GK, MEF, ND, ES; Supervision: ES.

Disclosure of conflicts of interest

This work was partly supported by a research grant from Servier laboratories. Several co-authors (LKB, SB, AD) are employees in this company.

References

1. Reynaud D, Pietras E, Barry-Holson K, *et al.* IL-6 controls leukemic multipotent progenitor cell fate and contributes to chronic myelogenous leukemia development. *Cancer Cell.* 2011;20(5):661-73.
2. Welner RS, Amabile G, Bararia D, *et al.* Treatment of chronic myelogenous leukemia by blocking cytokine alterations found in normal stem and progenitor cells. *Cancer Cell.* 2015;27(5):671–681.
3. Arber DA, Orazi A, Hasserjian R, *et al.* The 2016 revision to the World Health Organization classification of myeloid neoplasms and acute leukemia. *Blood.* 2016;127(20):2391-405.
4. Deininger MWN, Tyner JW, Solary E. Turning the tide in myelodysplastic/myeloproliferative neoplasms. *Nat Rev Cancer.* 2017;17(7):425-440.
5. Zhang Q, Zhao K, Shen Q, *et al.* Tet2 is required to resolve inflammation by recruiting Hdac2 to specifically repress IL-6. *Nature.* 2015;525(7569):389-393.
6. Cai Z, Kotzin JJ, Ramdas B, *et al*. Inhibition of Inflammatory Signaling in Tet2 Mutant Preleukemic Cells Mitigates Stress-Induced Abnormalities and Clonal Hematopoiesis. *Cell Stem Cell.* 2018;23(6):833-849.e5.
7. De Witte T, Bowen D, Robin M, *et al*. Allogeneic hematopoietic stem cell transplantation for MDS and CMML: recommendations from an international expert panel. *Blood.* 2017;129(13):1753-1762.
8. Merlevede J, Droin N, Qin T, *et al.* Mutation allele burden remains unchanged in chronic myelomonocytic leukaemia responding to hypomethylating agents. *Nat Commun.* 2016;7:10767.
9. Solary E and Itzykson R. How I treat chronic myelomonocytic leukemia. *Blood.* 2017;130(2):126-136
10. Patnaik MM, Sallman DA, Mangaonkar A, *et al.* Phase 1 study of lenzilumab, a recombinant anti-human GM-CSF antibody, for chronic myelomonocytic leukemia (CMML). *Blood.* 2020; blood.2019004352.
11. Selimoglu-Buet D, Wagner-Ballon O, Saada V, *et al.* Characteristic repartition of monocyte subsets as a diagnostic signature of chronic myelomonocytic leukemia. *Blood.* 2015;125(23):3618-26.
12. Itzykson R, Kosmider O, Renneville A, *et al.* Clonal architecture of chronic myelomonocytic leukemias. *Blood.* 2013;121(12):2186-98.
13. Wang X, Li T, Wang W, *et al.* Cytokine-like 1 Chemoattracts Monocytes/Macrophages via CCR2. *J Immunol.* 2016;196(10):4090-9.
14. Kotschy A, Szlavik Z, Murray J, *et al.* The MCL1 inhibitor S63845 is tolerable and effective in diverse cancer models. *Nature.* 2016;538(7626):477-482.
15. Vo TT, Ryan J, Carrasco R, *et al*. Relative mitochondrial priming of myeloblasts and normal HSCs determines chemotherapeutic success in AML. *Cell.* 2012;151(2):344-55.
16. Bencheikh L, Diop MK, Rivière J, *et al.* Dynamic gene regulation by nuclear colony-stimulating factor 1 receptor in human monocytes and macrophages. *Nat Commun.* 2019;10(1):1935
17. Selimoglu-Buet D, Rivière J, Ghamlouch H, *et al.* A miR-150/TET3 pathway regulates the generation of mouse and human non-classical monocyte subset. *Nat Commun.* 2018;9(1):5455.
18. Zhang Y, He L, Selimoglu-Buet D, *et al.* Engraftment of chronic myelomonocytic leukemia cells in immunocompromised mice supports disease dependency on cytokines. *Blood Adv.* 2017;1(14):972-979.
19. Yoshimi A, Balasis ME, Vedder A, *et al.* Robust patient-derived xenografts of MDS/MPN overlap

syndromes capture the unique characteristics of CMML and JMML. *Blood.* 2017;130(4):397-407.

20. Franzini A, Pomicter AD, Yan D, *et al.* The transcriptome of CMML monocytes is highly inflammatory and reflects leukemia-specific and age-related alterations. *Blood Adv.* 2019;3(20):2949-2961.

21. Lucas N, Duchmann M, Rameau P, et al. Biology and prognostic impact of clonal plasmacytoid dendritic cells in chronic myelomonocytic leukemia. *Leukemia* 2019;33(10):2466-2480.

22. Fishilevich S, Nudel R, Rappaport N, , *et al*. GeneHancer: genome-wide integration of enhancers and target genes in GeneCards. *Database* 2017 Jan 1;2017:bax028. doi: 10.1093/database/bax028.

23. Guha M, O'Connell MA, Pawlinski R, *et al.* Lipopolysaccharide activation of the MEK-ERK1/2 pathway in human monocytic cells mediates tissue factor and tumor necrosis factor alpha expression by inducing Elk-1 phosphorylation and Egr-1 expression. *Blood.* 2001;98(5):1429-39.

24. Kloos A, Mintzas K, Winckler L, et al. Effective drug treatment identified by in vivo screening in a transplantable patient-derived xenograft model of chronic myelomonocytic leukemia. Leukemia. 2020;34(11):2951-2963.

25. Kozopas KM, Yang T, Buchan HL, *et al.* MCL1, a gene expressed in programmed myeloid cell differentiation, has sequence similarity to BCL2. *Proc Natl Acad Sci U S A.* 1993;90(8):3516-20

26. Liu X, Rapp N, Deans R, *et al.* Molecular cloning and chromosomal mapping of a candidate cytokine gene selectively expressed in human CD34+ cells. *Genomics.* 2000;65(3):283-92.

27. Gupta VA, Matulis SM, Conage-Pough JE, *et al*. Bone marrow microenvironment-derived signals induce Mcl-1 dependence in multiple myeloma. *Blood*. 2017;129(14):1969-1979.

28. Beroukhim R, Mermel CH, Porter D, *et al.* The landscape of somatic copy-number alteration across human cancers. *Nature.* 2010;463(7283):899-905.

29. Ten Hacken E, Valentin R, Regis FFD, *et al.* Splicing modulation sensitizes chronic lymphocytic leukemia cells to venetoclax by remodeling mitochondrial apoptotic dependencies. *JCI Insight.* 2018;3(19).

30. Merino D, Kelly GL, Lessene G, *et al*. BH3-Mimetic Drugs: Blazing the Trail for New Cancer Medicines. *Cancer Cell.* 2018;34(6):879-891.

31. Elgendy M, Abdel-Aziz AK, Renne SL, *et al*. Dual modulation of MCL-1 and mTOR determines the response to sunitinib. *J Clin Invest.* 2017;127(1):153-168.

32. Fiskus W, Cai T, DiNardo CD, *et al.* Superior efficacy of cotreatment with BET protein inhibitor and BCL2 or MCL1 inhibitor against AML blast progenitor cells. *Blood Cancer J* 2019;9(2):4.

33. Merino D, Whittle JR, Vaillant F, *et al.* Synergistic action of the MCL-1 inhibitor S63845 with current therapies in preclinical models of triple-negative and HER2-amplified breast cancer. *Sci Transl Med.* 2017;9(401).

34. Yamaguchi R, Lartigue L, Perkins G. Targeting Mcl-1 and other Bcl-2 family member proteins in cancer therapy. *Pharmacol Ther.* 2019;195:13-20.

35. Inoue-Yamauchi A, Jeng PS, Kim K, *et al.* Targeting the differential addiction to anti-apoptotic BCL-2 family for cancer therapy. *Nat Commun.* 2017;8:16078.

36. Shastri A, Choudhary G, Teixeira M, *et al.* Antisense STAT3 inhibitor decreases viability of myelodysplastic and leukemic stem cells. *J Clin Invest.* 2018;128(12):5479-5488.

37. Kim JS, Ryoo ZY, Chun JS. Cytokine-like 1 (Cytl1) regulates the chondrogenesis of mesenchymal cells. *J Biol Chem.* 2007;282(40):29359-67.

38. Chao C, Joyce-Shaikh B, Grein J, *et al.* C17 prevents inflammatory arthritis and associated joint destruction in mice. *PLoS One.* 2011;6(7):e22256.

39. Tomczak A, Singh K, Gittis AG, *et al*. Biochemical and biophysical characterization of cytokine-like protein 1 (CYTL1). *Cytokine.* 2017;96:238-246.

40. Niyongere S, Lucas N, Zhou JM, *et al.* Heterogeneous expression of cytokines accounts for clinical diversity and refines prognostication in CMML. *Leukemia.* 2019;33(1):205-216.

41. de Zeeuw D, Bekker P, Henkel E, *et al.* CCX140-B Diabetic Nephropathy Study Group The effect of CCR2 inhibitor CCX140-B on residual albuminuria in patients with type 2 diabetes and nephropathy: a randomised trial. *Lancet Diabetes Endocrinol.* 2015;3(9):687-96.

42. Nywening TM, Wang-Gillam A, Sanford DE, *et al.* Targeting tumour-associated macrophages with CCR2 inhibition in combination with FOLFIRINOX in patients with borderline resectable and locally advanced pancreatic cancer: a single-centre, open-label, dose-finding, non-randomised, phase 1b trial. *Lancet Oncol.* 2016;17(5):651-62.

43. D'Antoni ML, Paul RH, Mitchell BI, *et al.* Improved Cognitive Performance and Reduced Monocyte Activation in Virally Suppressed Chronic HIV After Dual CCR2 and CCR5 Antagonism. *J Acquir Immune Defic Syndr.* 2018;79(1):108-116.

44. Koschmieder S, Mughal TI, Hasselbalch HC, *et al.* Myeloproliferative neoplasms and inflammation: whether to target the malignant clone or the inflammatory process or both. *Leukemia.* 2016;30(5):1018-24.

45. Brinkmann K, Grabow S, Hyland CD, *et al*. The combination of reduced MCL-1 and standard chemotherapeutics is tolerable in mice. *Cell Death Differ.* 2017;24(12):2032-2043.

46. Kunimoto H, Meydan C, Nazir A, *et al*. Cooperative Epigenetic Remodeling by TET2 Loss and NRAS Mutation Drives Myeloid Transformation and MEK Inhibitor Sensitivity. *Cancer Cell* 2018;33(1):44-59.e8

Sevin M, Debeurme F et al, Table 1

	Patients
Number of cases	190
Mean age in years (range)	74.3 (28-100)
Sex ratio M/F	111/74
CMML 0/1/2 (WHO classification)	82/50/43
Proliferative/Dysplastic	89/81
Leucocytes, mean 10^9/L (range)	20.8 (3.8-137.3)
Monocytes, mean 10^9/L (range)	4.7 (0.4-29.9)
Platelet count, mean 10^9/L (range)	156.3 (14-996)
Hemoglobin level, mean g/dL (range)	11.6 (6.8-16.8)
Karyotype (N/A/ND)	116/33/41
Main genetic alterations	
TET2	124/173 (72%)
SRSF2	63/161 (39%)
ASXL1	72/173 (42%)
NRAS	29/172 (17%)
KRAS	24/172 (14%)
CBL	15/172 (9%)

Table 1. Characteristic of CMML patients included in the trial. Samples from a given patient were used for several independent experiments (see table S2) and serial sampling was performed in some patients. A total number of 246 samples collected from 190 patients were tested. M, male; F, female; CMML, chronic myelomonocytic leukemia; Karyotype: N, normal; A, Abnormal; NA, not available.

Figure legends

Figure 1. Defective apoptosis of CMML peripheral blood monocytes. A. Cell viability of $CD14^+$ monocytes sorted from CMML patients (n=16) and healthy donors (n=27) peripheral blood was analyzed by Trypan blue dye exclusion after 4 days in culture without serum. Mann-Whitney test. ***P<0.001. **B.** $CD14^+$ monocytes were sorted from CMML patient (n=21) and healthy donors (n=30) peripheral blood and stained with annexin V-FITC (AnV) and propidium iodide (PI) after 4 days in culture without serum; the AnV^+/PI^- fraction was measured by flow cytometry. Mann-Whitney test. ****P<0.0001. **C.** AnV^+/PI^- fraction of $CD14^+$ monocytes sorted from CMML patient (n=78) and healthy donors (n=102) peripheral blood as determined by flow cytometry after 24 hours in culture in the presence of 10% fetal calf serum. Mann-Whitney test. ****P<0.0001. **D,E.** Patient samples tested in Figure 1C were classified according to patients characteristics, including the 2016 iteration of the WHO classification separating CMML-0 from CMML-1 and CMML-2 (**D**) and the presence or absence of mutations in the indicated genes (**E**).

Figure 2. CMML monocyte addiction to MCL1. A. Intracellular BH3 (iBH3) profiling: $CD14^+$ peripheral blood monocytes collected from CMML patients (in blue, n=14-21) and healthy donors (in red, n=17-22) were incubated with indicated peptides (80 µM) before flow measurement of the fraction of cytochrome c released. **B.** RT-qPCR analysis of indicated gene expression in sorted peripheral blood monocytes collected from CMML patients (in blue, n=9-30) and healthy donors (in red, n=9-28), using *PPIA* as a housekeeping gene. Mean ± SEM. Mann-Whitney test. * P<0.05; ** P<0.01; *** P<0.001; **C.** Peripheral blood monocytes from CMML patients (n=24-71) and healthy donors (n=12-49) were treated with venetoclax (1 µM), navitoclax (100 nM), or S63845 (10 nM) for 24 hours at 37°C before measuring the fraction of annexin-V-negative, propidium iodide negative cells by flow cytometry. **P<0.01, ns, not significant (Mann-Whitney test). **D.** Immunoblot analysis of indicated proteins in sorted monocytes treated with indicated doses of S63845 for 24 hours.

Figure 3. Overexpression of CYTL1 in CMML monocytes. A. Volcanoplot analysis of differentially methylated regions identified by ERRBS by comparing CMML monocytes with defective (n=10) and non-defective (n=9) apoptosis, based on their survival after 24 hours in serum containing medium (> or ≤ 50%). **B.** GO pathway analysis of ERRBS data, identifying MAP3K as the most significant differentially regulated pathway. **C.** Volcanoplot analysis of

differentially expressed genes identified by RNA sequencing of samples analyzed in A. **D.** Healthy donor monocytes were incubated for 24 hours in culture medium with 10% peripheral blood plasma collected from healthy donors (red, n=4) or CMML patients (blue, n=19). The fraction of surviving cells (AnV^{neg}; IP^{neg}) was normalized to that of control monocytes in serum free medium. All panels, Mann-Whitney test. * P<0.05; **E.** CYTL1 gene expression measured by RT-qPCR in healthy donor (red) and CMML (blue) monocytes, using RPL32 as a housekeeping gene. Mann-Whitney test. ****P<0.0001. **F.** *CYTL1* gene expression analyzed in RNA sequencing data from Franzini et al, 2019 (ref 20). Kuskal-Wallis test, Dunn's multiple comparison, ** P<0.01. **G.** CYTL1 protein level measured in the peripheral blood plasma of healthy donors (red) and CMML (blue) patients. Mann-Whitney test. ** P<0.01.

Figure 4. Increased survival of monocytes through a CYTL-1/CCR2/MEK pathway. A. ChIP-seq analysis of *CYTL1* gene in healthy donor monocytes. H3K27me3, H3K4me1, H3K4me3, and H3K27ac ChIP-seq data were obtained *in silico*. ChIP-Seq of EGR1 was performed in two healthy donors and 2 CMML monocyte samples. Dotted rectangle indicates a suspected gene enhancer, based on histone marks repartition. **B.** ChIP-qPCR analysis of EGR1 enrichment on *CYTL1* enhancer using 2 sets of primers (Enh Set1 and 2) in CMML monocytes with low (similar to controls) or high (as compared to control, see figure 3E) *CYTL1* gene expression; in blue, CMML#1 and #2 shown in panel A. **C.** Immunoblot analysis of indicated proteins (P-ERK = ERK phosphorylated on thr202 and tyr 204) in cells treated for with 100 ng/ml rhCYTL1 for 15 minutes or 8 nM CAS 445 for 30 minutes or both. Actin is used as a loading control. Lower panel: quantification of the above imunoblot. **D.** Healthy donor monocytes were incubated for 24 hours with or without 100 ng/ml CYTL1, before measuring the surviving fraction of cells by flow cytometry (AnV^{neg}; IP^{neg}, results normalized to control monocytes). Mann-Whitney test. ****P<0.0001. **E.** Healthy donor monocytes were incubated for 24 hours with 100 ng/ml CYTL1 in the absence or presence of CAS 445479-97-0 (8nM) or RS 504393 (10µM) before measuring the surviving fraction of cells by flow cytometry (AnV^{neg}; IP^{neg}, results normalized to CYTL1 alone). Kuskal-Wallis test, Dunn's multiple comparison, * P<0.05; ** P<0.01.

Figure 5. S63845 / MEK inhibitor combination induced CMML monocyte apoptosis. A,B. Sorted monocytes from healthy donor (grey) or CMML patients (colors) were treated for 10 nM S63845, 100 nM AZD6244 (AZD, selumetinib) (**A**) or 10 nM trametinib (TRAM) (**B**) or their

combination for 24 hours before measuring the surviving fraction of cells (AnV^{neg}; IP^{neg}) by flow cytometry (results are normalized to cells treated with DMSO alone). Mann-Whitney test. ***P*<0.01; ****P*<0.001; *****P*<0.0001. **C.** Immunoblot analysis of indicated proteins in CMML patient monocytes treated for 24 hours as in A,B. **D.** Quantification of the P-ERK/ERK and MCL1/ACTIN ration using imageQuant LAS 4000 camera and ImageJ software on indicated numbers of immunoblots. **E.** Immunoblot analysis of indicated proteins in 4 CMML patient monocytes treated for 4 hours as in A,B (using imageQuant LAS 4000 camera and ImageJ software (When multiple samples analyses, mean ± SEM).

Figure 6. The S63845 / MEK inhibitor combination decreases leukemic infiltration in CMML PDX models. **A.** Experimental plan of PDX models obtained by iv injection of 0.4 x 10^6 $CD34^+$ sorted cells (**B,C**) or 3.5 x 10^6 bone marrow mononucleated cells (**E**), 7 weeks before starting treatment with S63845 (20 mg/kg iv once a week for 3 weeks) and gavage with either selumetinib, 10 mg/kg (**B,C**) or trametinib 1 mg/kg (**E**) 5 days a week for 3 weeks. **B.** Photographs of spleen size in 4 mice treated with vehicle or the S63845/selumetinib combo. **C.** Impact of the S63845/selumetinib combo on spleen weight, the absolute number of human $CD45^+$ and $CD45^+$,$CD14^+$ cells detected in the spleen, and the number of human cells per microliter of peripheral blood. Results of two independent PDX models are mixed (vehicle, n=13; combo, n=15). **D.** Plasma level of indicated human cytokine measured in the peripheral blood plasma of mice treated as in C. * *P*<0.05; ** *P*<0.01; *** *P*<0.001 (Mann-Whitney test).**E.** Impact of the S63845, trametinib and their combination (n=8 per group) on spleen weight, the absolute number of human cells detected in the spleen or the bone marrow and the number of human cells per microliter of peripheral blood.

Sevin M, Debeurme F et al, Figure 1

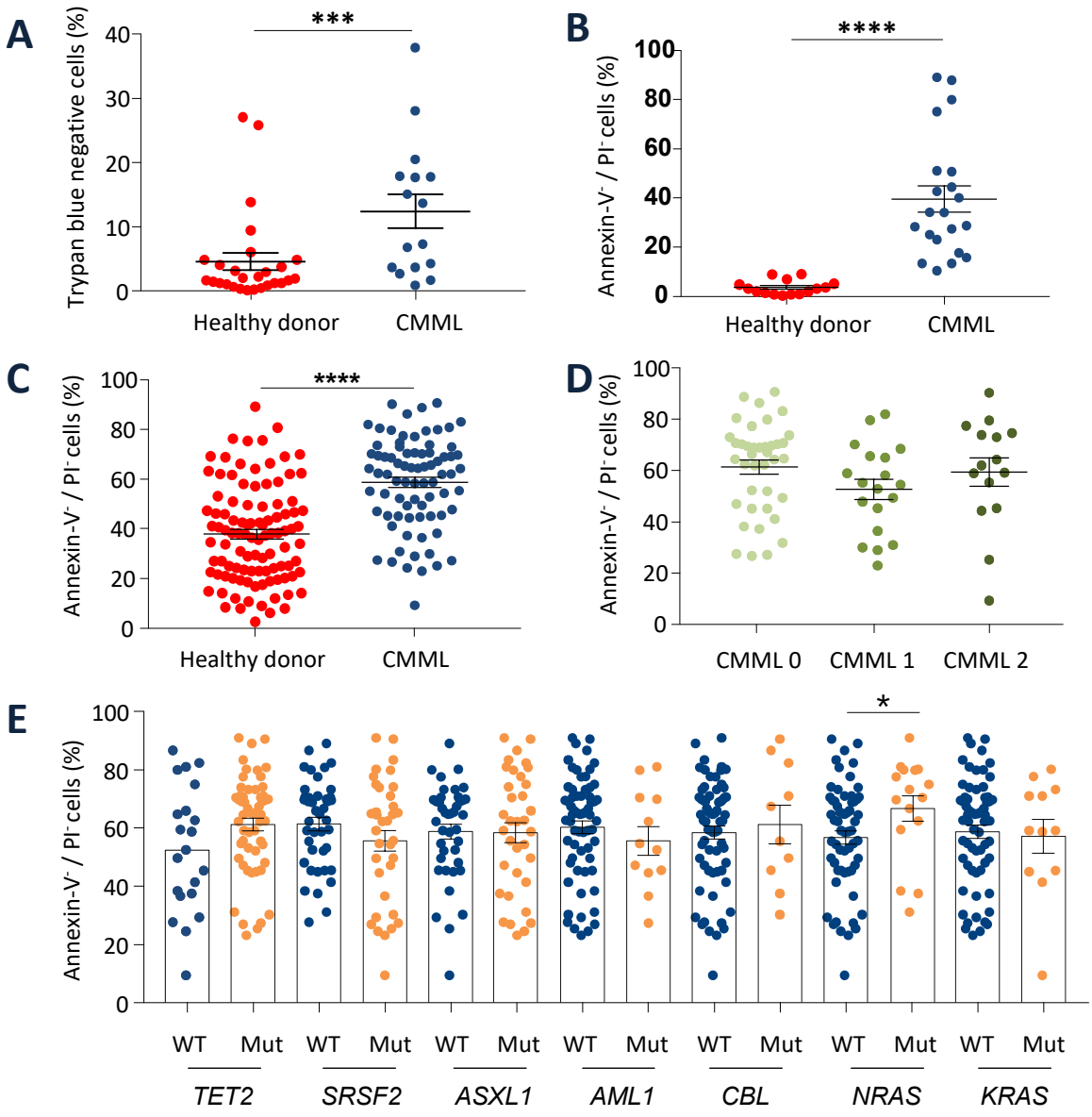

Sevin M, Debeurme F, Figure 2

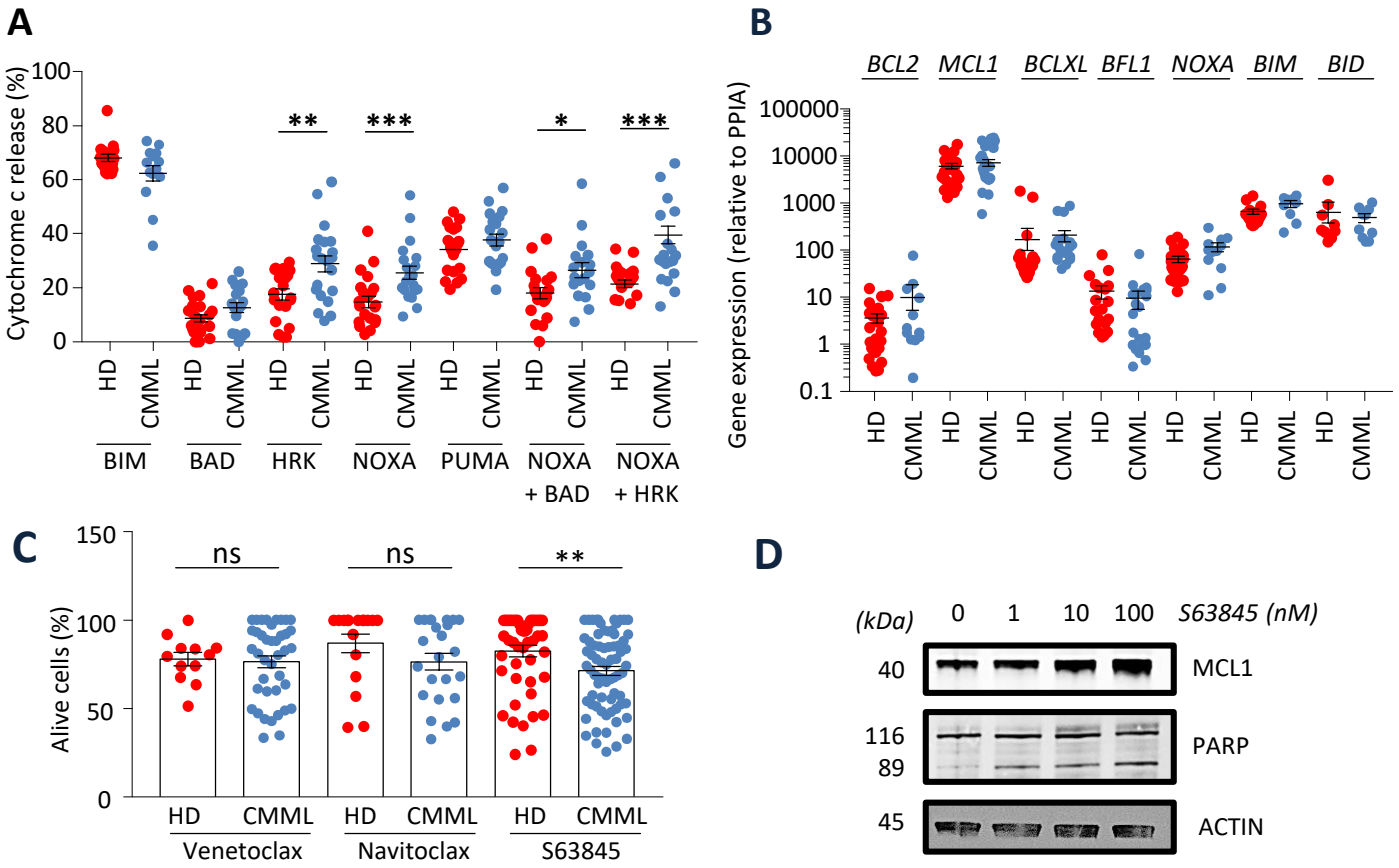

Sevin M, Debeurme F et al, Figure 3

A

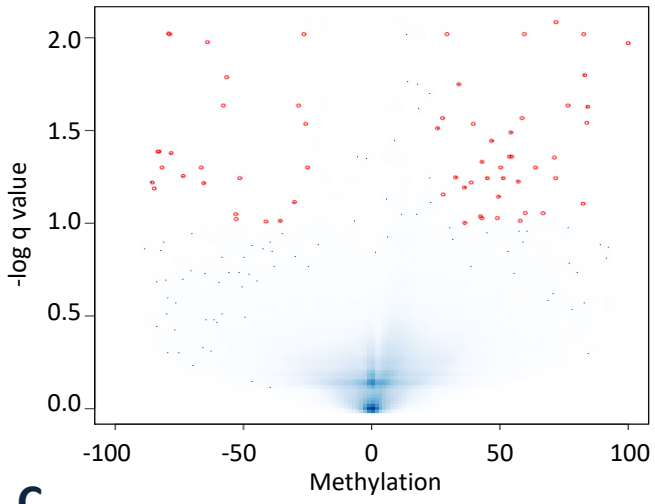

B

Geneset.ID	Description	FDR
GO:0031435	mitogen-activated protein kinase kinase kinase binding	0.000
GO:0043425	bHLH transcription factor binding	0.001
GO:0016893	endonuclease activity, active with either RNA or DNA	0.011
GO:0005158	Insulin receptor binding	0.024

C

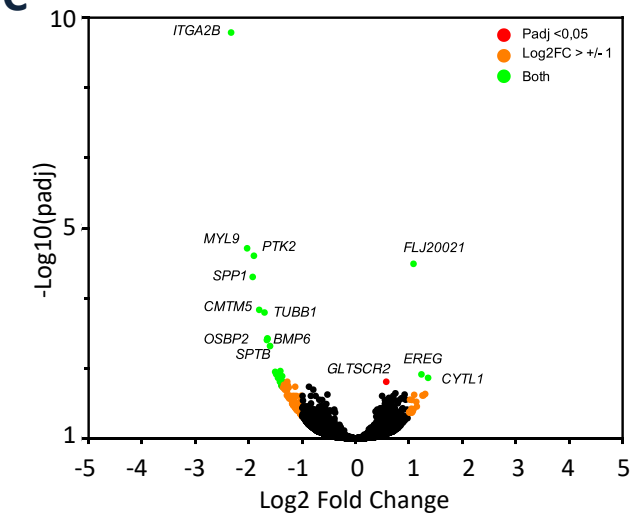

D

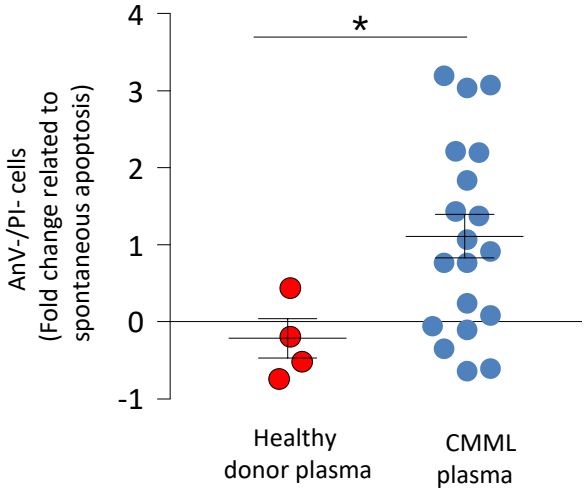

E

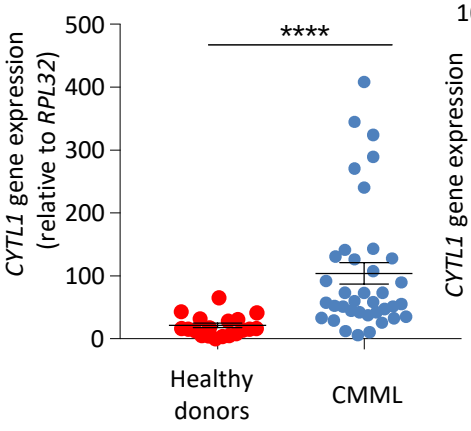

F

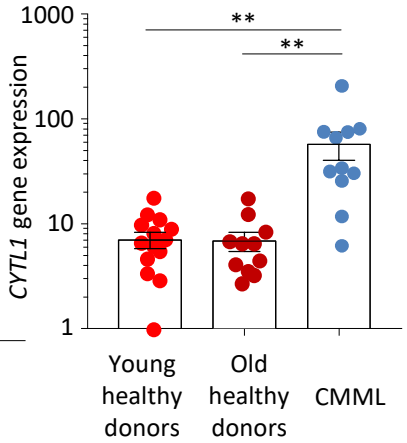

G

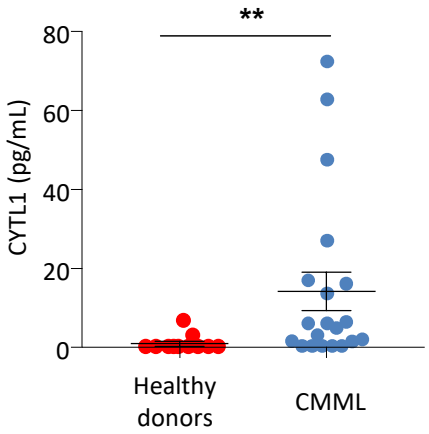

Sevin M, Debeurme F, Figure 4

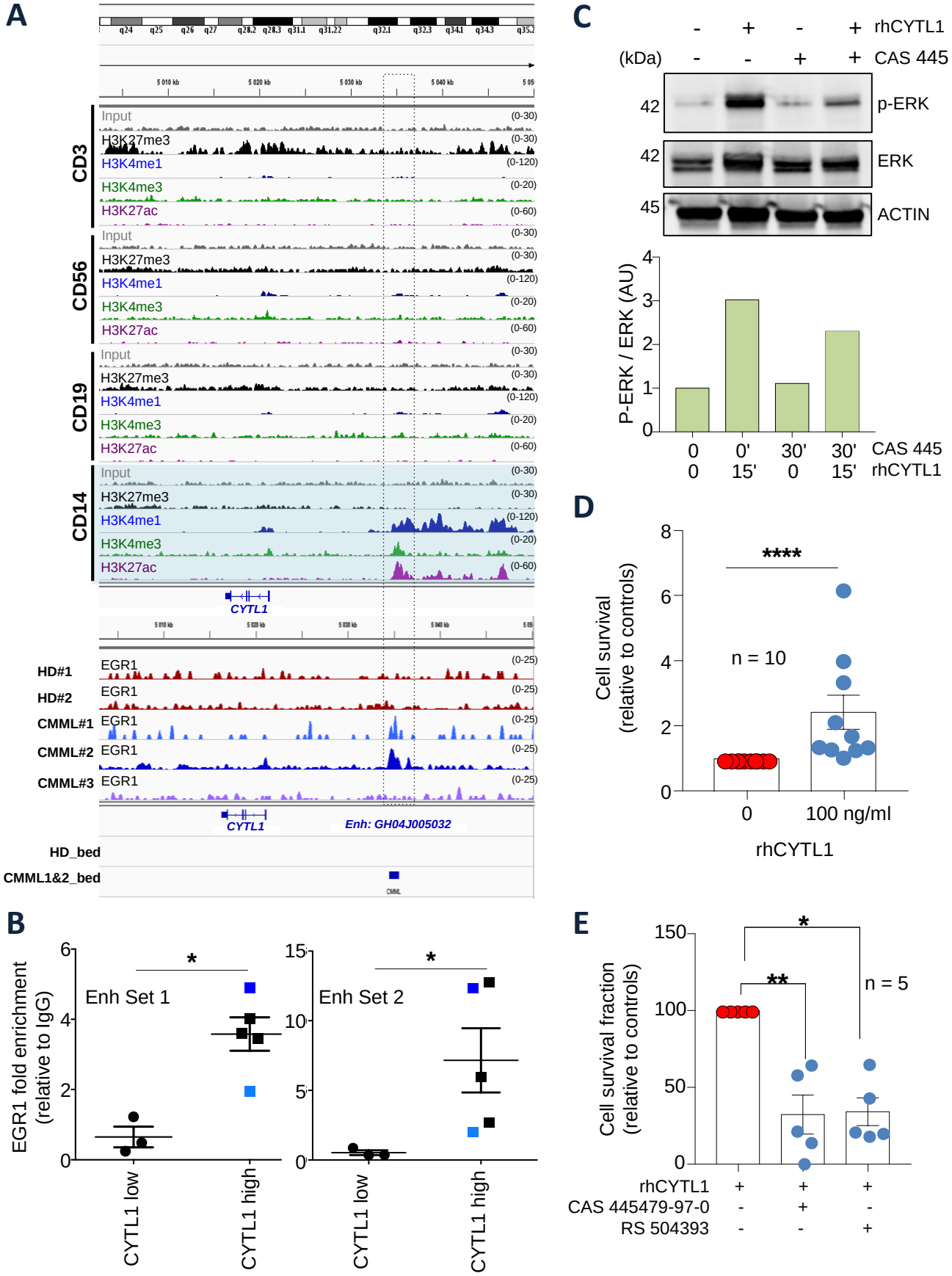

Sevin M and Debeurme F, Figure 5

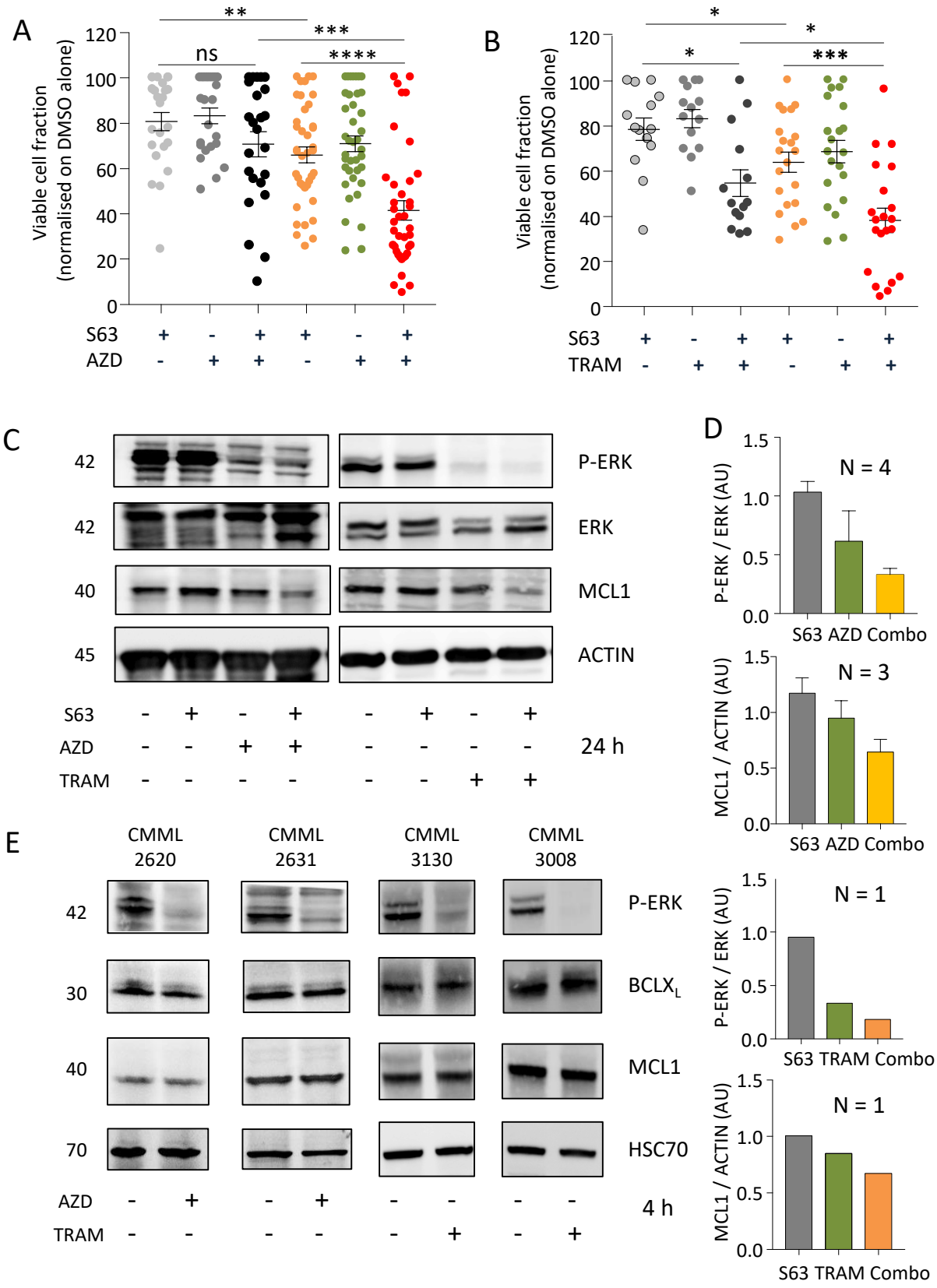

Sevin M, Debeurme F et al, Figure 6